

# A mammalian oocyte-specific linker histone gene *H1oo*: homology with the genes for the oocyte-specific cleavage stage histone (*cs-H1*) of sea urchin and the *B4/H1M* histone of the frog

Mamoru Tanaka\*, Jon D. Hennebold†, Jane Macfarlane and Eli Y. Adashi§

Division of Reproductive Sciences, Department of Obstetrics and Gynecology, University of Utah Health Sciences Center, Salt Lake City, UT 84132, USA

\*Present address: Department of Obstetrics and Gynecology, Keio University School of Medicine, 35 Shinanomachi, Shinjuku-ku, Tokyo 160-0082, Japan

†Present address: Oregon Regional Primate Research Center, Oregon Health Sciences University, 505 N.W. 185th Avenue, Beaverton, OR 97006, USA

§Author for correspondence (e-mail: eadashi@hsc.utah.edu)

Accepted 7 December 2000; published on WWW 7 February 2001

## SUMMARY

Oocytes and early embryos of multiple (non-mammalian) species lack the somatic form of the linker histone H1. To the best of our knowledge, a mammalian oocyte-specific linker (H1) histone(s) has not, as yet, been reported. We have uncovered the cDNA in question in the course of a differential screening (suppression subtractive hybridization (SSH)) project. Elucidation of the full-length sequence of this novel 1.2 kb cDNA led to the identification of a 912 bp open reading frame. The latter encoded a novel 34 kDa linker histone protein comprised of 304 amino acids, tentatively named *H1oo*. Amino acid BLAST analysis revealed that *H1oo* displayed the highest sequence homology to the oocyte-specific B4 histone of the frog, the respective central globular (putative DNA binding) domains displaying 54% identity. Substantial homology to the *cs-H1* protein of the sea urchin oocyte was also apparent. While most oocyte mRNAs corresponding to somatic linker histones are not polyadenylated (and remain

untranslated), the mRNAs of (non-mammalian) oocyte-specific linker histones and of mammalian *H1oo*, are polyadenylated, a process driven by the consensus signal sequence, AAUAAA, detected in the 3'-untranslated region of the *H1oo* cDNA. Our data suggest that the mouse oocyte-specific linker histone *H1oo* (1) constitutes a novel mammalian homolog of the oocyte-specific linker histone B4 of the frog and of the *cs-H1* linker histone of the sea urchin; (2) is expressed as early as the GV (PI) stage oocyte, persisting into the MII stage oocyte, the oocyte polar bodies, and the two-cell embryo, extinction becoming apparent at the four- to eight-cell embryonic stage; and (3) may play a key role in the control of gene expression during oogenesis and early embryogenesis, presumably through the perturbation of chromatin structure.

Key words: Oocyte-specific linker histone, Mouse, Oocyte, Maternal mRNA, *H1oo*, Frog, Sea urchin

## INTRODUCTION

The DNA of eukaryotes is packed along with histone proteins into chromatin. There exist two types of histone proteins: the core histones (H2A, H2B, H3 and H4) and the linker histones such as H1 (Doenecke et al., 1997; Wolffe, 1998). The core histones constitute a component of the nucleosome core particle, an octamer of core histones intertwined with a 146 bp DNA stretch defined by its resistance to digestion even after extensive micrococcal nuclease cleavage. The linker histones, in turn, constitute the major proteins bound, in part, to linker DNA, the DNA-bridging nucleosome core particles. The composition of the linker histone fraction is tissue and species specific, as well as developmentally regulated (Doenecke et al., 1997; Wolffe, 1998). As such, linker histones play a crucial role in the higher-order packaging of chromatin and, thus, inevitably in an impressive array of regulatory functions. A recent report in the frog has suggested that in vitro replacement

of the oocyte-specific linker histone B4 by its somatic H1 counterpart may lead to spatial chromosomal reorganization designed to occlude the binding site for the critical transcription factor TFIIIA (Crane-Robinson, 1999).

Alterations in the type and expression level of the histone family complement during oogenesis and embryogenesis are highly regulated in many organisms. This process has been most extensively studied in the sea urchin, wherein different sets of histone genes are sequentially expressed during early development. Unfertilized sea urchin oocytes synthesize a large maternal pool of linker histones known as cleavage-stage histones H1 (*cs-H1*). This trend continues throughout the early stages of embryogenesis at which time *cs-H1* is the only linker histone present in chromatin (Childs et al., 1982; Herlands et al., 1982). However, *cs-H1* biosynthesis continues for only a brief period after fertilization. A similar developmentally-regulated transition occurs in the frog. The *Xenopus laevis* B4 (or H1M) protein constitutes a linker histone of the H1 subtype

the expression of which is restricted to early developmental stages. Specifically, B4 accumulates during oogenesis, persisting until near the mid-blastula transition when it is replaced by somatic linker histone H1 subtypes (Dimitrov et al., 1994; Dimitrov and Wolffe, 1996). Based on the sequence similarity of the proteins in question, as well as their expression pattern, it has been proposed that the cs-H1 and B4 proteins constitute trans-species homologs (Clarke et al., 1998; Mandl et al., 1997). The absence of immunoreactive somatic H1 histones in fully grown mammalian oocytes and early embryos, as indicated by immunofluorescence and immunoblotting, implies that this histone species is all but absent during oogenesis and early embryogenesis (Clarke et al., 1997; Stein and Schultz, 2000). Indeed, the somatic histone H1 first becomes detectable in chromatin at the two-cell stage, a time when the embryonic genome becomes transcriptionally active (Stein and Schultz, 2000). Clearly then, an oocytic-embryonic switch in the linker histone subtype is likely to occur during mammalian embryogenesis as well. To date, no evidence has been offered to document the existence of a mammalian oocyte-specific (maternally derived) linker histone homologous to the cs-H1 of sea urchin and/or to the B4 of the frog.

We have aimed to characterize one such maternal transcript that was isolated in our laboratory from the mouse ovary by differential screening technology.

## MATERIALS AND METHODS

### In vivo protocols: superovulation

Female C57BL/6 mice, purchased from Jackson Laboratories (Bar Harbor, ME), 19 days of age upon arrival, were initially quarantined for 3 days at the University of Utah Animal Resources Center. The latter adheres to the guidelines outlined by The Animal Welfare Act and to Institutional Animal Care and Use Committee (IACUC) protocols. At 25 days of age, one group of mice ( $n=8$ ) was sacrificed by Halothane-induced asphyxiation (Halocarbon, River Edge, NJ), thereby providing unstimulated ovarian material as well as non-ovarian tissues. A second group of mice ( $n=37$ ) was injected with 10 IU each of pregnant mare serum gonadotropin (PMSG). 48 hours after the PMSG injection, a group of mice ( $n=7$ ) was sacrificed so as to secure ovaries at the preovulatory phase of the reproductive cycle. The remaining mice ( $n=30$ ) were injected with 10 IU each of human chorionic gonadotropin (hCG). Subgroups ( $n=5$ /subgroup) of the latter were sacrificed at 3, 6, 9, 12, 24 and 48 hours post-hCG injection. Ovaries removed 3, 6, 9 and 12 hours post-hCG encompass the ovulatory interval preceding follicular rupture whereas the 24 and 48 hours post-hCG treatment groups encompass the postovulatory phase of the ovarian cycle.

### Collection of oocytes and embryos

C57BL/6 female mice, 3-5 weeks of age, were superovulated as described earlier. GV-stage oocytes were collected by puncturing mouse follicles 44-48 hours after PMSG injection with 30-gauge needles. Unfertilized metaphase II (MII) oocytes were collected at 16 hours post-hCG from the incised oviductal ampullae of superovulated/unmated mice. Fertilized one-cell embryos were collected 24 hours post-hCG from the incised oviductal ampullae of superovulated/mated female mice. Mating was carried out with the same strain of males. The adherent cumulus cells and the sperm were removed from one-cell embryos by digestion with 1% hyaluronidase (Sigma, St. Louis, MO) for  $\leq 5$  minutes. Two-cell embryos were obtained 41-42 hours post-hCG by flushing the oviducts of

superovulated/mated female mice. Advanced stage embryos were obtained by further culturing of two-cell stage embryos. In this case, the two-cell embryos were transferred to Hepes-buffered D-MEM medium supplemented with Earle's balanced solution, essential amino acids (GIBCO-BRL, Grand Island, NY), 110mg/l sodium pyruvate, 75 mg/l penicillin G, 50 mg/l streptomycin and 0.5% BSA (Sigma). Embryo cultures were carried out in an incubation chamber, equilibrated with 5% CO<sub>2</sub> and air, and maintained at 37°C. Thus, two-cell-, four-cell-, and eight-cell-stage embryos were collected 41-42, 63-64 and 73-74 hours post hCG treatment, respectively.

### Total RNA isolation

Total RNA was isolated from the following non-ovarian tissues of immature 25-day-old female C57BL/6 mice: brain, heart, kidney, liver, spleen and lung. Total RNA was also isolated from the ovaries of 25-day-old female C57BL/6 mice undergoing superovulation as described above. The isolation of total RNA was performed using Qiagen's RNeasy Kit (Santa Clara, CA) as per the manufacturer's directions. PolyA<sup>+</sup> RNA was subsequently isolated by the use of an oligo-dT/magnetic sphere-based separation system (RNAtract, Promega, Madison, WI).

### Suppression subtractive hybridization (SSH) and cloning of cDNA

SSH was performed as described before (Hennebold et al., 2000). Briefly, an equal amount of PolyA<sup>+</sup> RNA, isolated from each of the non-ovarian tissues, was combined to generate a total of 1  $\mu$ g of PolyA<sup>+</sup> RNA. This mRNA was used to generate the 'driver' cDNA through the use of the SMART cDNA synthesis kit (Clontech, San Diego, CA) according to the manufacturer's instructions. Ovarian PolyA<sup>+</sup> RNA (1  $\mu$ g), isolated from mice undergoing the above-described superovulation protocol, was used to construct the 'tester' cDNA. The latter, in effect, represented the totality of the ovarian life cycle by virtue of the pooling of all samples, i.e. untreated, post-PMSG and post-hCG. 30 primary and 12 secondary PCR cycles were used in amplifying the 'target' (subtracted) putative ovary-selective cDNAs. The PCR products (partial cDNAs) generated by SSH were ligated into the vector pCR-SCRIPT (Stratagene, San Diego, CA) and sequenced. The sequence data were analyzed for homology to previously characterized genes deposited in GenBank, DataBank of Japan (DDB) and the European Molecular Biology Laboratory (EMBL) using the BLAST nucleotide program.

### Northern blot analysis

Total RNA (20  $\mu$ g) isolated from ovaries at different stages of the superovulation protocol was separated on denaturing 1% agarose-formaldehyde gels and transferred to Nylon membranes as described elsewhere (Hennebold et al., 2000). Prior to transfer, RNA quality and concentration was assessed by ethidium bromide staining followed by visualization under UV light. Non-ovarian tissue blots (20  $\mu$ g of total RNA), in turn, were purchased from Origene Technologies (Rockville, MD). The above nylon membranes were pre-hybridized for 2-6 hours at 42°C in 5 $\times$  SSPE, 50% formamide, 5 $\times$  Denhardt's and 0.25% SDS. Probes were generated by radiolabeling individual (SSH-derived) PCR-amplified cDNA inserts with [<sup>32</sup>P]-dCTP with the random-priming method (Amersham Pharmacia, Piscataway, NJ). The above probes were denatured in a boiling water bath for 5 minutes prior to quenching with ice. Membranes were hybridized overnight at 42°C with the relevant probe in the same (above mentioned) solution used for pre-hybridization. Thereafter, membranes were washed 3 times with 2 $\times$  SSC and 0.1% SDS at room temperature for 5 minutes, followed by 2 washes with 0.125 $\times$  SSC and 0.25% SDS at 60°C for 15 minutes. The blots were then rinsed in 4 $\times$  SSC and imaged with a phosphorimager (BioRad, Hercules, CA). The intensity of the signals was quantified using Molecular Analyst® software (BioRad, Hercules, CA). Equivalent RNA loading was verified by probing the same (stripped) blots with radiolabeled PCR products of the

housekeeping genes for  $\beta$ -actin (*Actb* – Mouse Genome Informatics; in the case of ovarian blots) and glyceraldehyde-3-phosphate dehydrogenase (*Gapd* – Mouse Genome Informatics; in the case of non-ovarian tissue blots).

### Cloning of the full-length cDNA corresponding to the SSH-generated partial cDNA: construction of a mouse cDNA library

A mouse ovary cDNA library was constructed using the SMART cDNA Library Construction Kit (Clontech, San Diego, CA) as per the manufacturer's directions. Briefly, ovarian RNA isolated from mice undergoing the above-described superovulation protocol was mixed with SMART III oligonucleotide, CDS III/3' PCR primer and MMLV reverse transcriptase to generate first-strand cDNAs. Primer-extended ds-cDNA was digested with *Sfi*I and ligated to lambda TriplEx2 vector. Recombinant phages ( $\sim 10^6$ ) comprising the mouse ovary cDNA library were screened with radiolabeled probes generated through random priming of the cloned (SSH-derived) PCR fragments. Positive clones were rescreened and plaque purified. Clones E121 and E81, the insert size of which was 1.2 kb, were chosen for DNA sequence analysis.

### RT-PCR analysis of oocytic and embryonic mRNA

Oocytes and embryos were collected, washed three times in Hepes-buffered D-MEM medium, transferred to a 1.5 ml tube containing 100  $\mu$ l of denaturing solution (Micro-RNA isolation kit: Stratagene, San Diego, CA) and vortexed. The samples were then spun down briefly and frozen at  $-80^\circ\text{C}$  prior to RNA purification. Total RNA was purified with the above-mentioned Micro-RNA isolation kit as per the manufacturer's protocol. Glycogen was employed as the carrier during the precipitation of the RNA. mRNAs were converted to cDNAs using the Sensiscript RT Kit (Quiagen, Santa Clara, CA) replete with the pd(T)<sub>12-18</sub> primer and the RNAGuard Ribonuclease Inhibitor (Amersham Pharmacia Biotech, Piscataway, NJ) according to the manufacturer's instructions. cDNAs derived from 15 embryos were used to amplify both the H1oo and  $\beta$ -actin cDNAs in 50  $\mu$ l of 10 mM Tris-HCl, 1.5 mM MgCl<sub>2</sub>, 50 mM KCl, 0.1% Triton X-100, 0.2 mM of each dNTP, 0.5 U of Taq polymerase and 0.5 mM of each primer. The PCR program consisted of 50 seconds incubation at  $94^\circ\text{C}$ , followed by 40 cycles at  $94^\circ\text{C}$  (35 seconds),  $59^\circ\text{C}$  (35 seconds) and  $72^\circ\text{C}$  (90 seconds). Aliquots, representing 10% of each amplicon, were run on 2.0% agarose gels. The H1oo primers were as follows: 295-317, 5'-CCACCCGTTTCAAGTACCTGTTG-3'; 554-533, 5'-CCTCCTTCTTGCCCTTCTCC-3'. The cytoskeletal  $\beta$ -actin (GenBank Accession Number: X03672) primers were based on the published cDNA sequence: 704-726, 5'-CGTGC GTGACATCAAAG-AGAAGC-3'; 1144-1121, 5'-ATCTGCTGGAAGGTGGACAGT-GAG-3'.

### Ovarian processing for histology, in situ hybridization and immunohistochemistry

Ovaries were surgically removed from 8-week old mice. The latter were fixed for 4 hours in 10% neutral formalin in PBS (pH 7.4) at room temperature, embedded in paraffin wax, and sectioned (6  $\mu$ m). Tissue sections were deparaffinized and rehydrated through xylene and a graded alcohol series. Following deparaffinization of the ovarian tissue sections in xylene, hydrated slides were digested with proteinase K (1  $\mu$ g/ml; Boehringer Mannheim, Mannheim, Germany) for 50 minutes at room temperature, fixed with 4% paraformaldehyde for 2 minutes, rehydrated, acetylated for 10 minutes in freshly prepared 0.25% acetic anhydride in 0.1 M triethanolamine (pH 8.0), dehydrated through graded ethanol (30-100%) and air-dried.

### In situ hybridization

The SSH-generated cDNA, ligated into the vector pCR-SCRIPT, was used to generate RNA probes for in situ hybridization. A digoxigenin (DIG)-labeled antisense RNA probe was obtained by using a *Bam*HI-

digested template, T3 RNA polymerase and a DIG RNA labeling kit (Boehringer Mannheim, Mannheim, Germany). A sense probe (negative control) was prepared using a *Nor*I-digested template, T7 RNA polymerase and the DIG RNA labeling kit. Slide-mounted ovarian sections were eventually hybridized with 1:100 dilution of the antisense or sense probe at  $55^\circ\text{C}$  for 16 hours in 50% formamide, 4 $\times$  SSC, 1 $\times$  Denhardt's solution, 10% dextran sulfate, 0.25 mg/ml yeast tRNA, and 0.5 mg/ml Salmon Sperm DNA. After hybridization, the slides were washed in 50% formamide/2 $\times$  SSC for 20 minutes at  $50^\circ\text{C}$  and the hybridized probe detected with an alkaline phosphatase-conjugated anti-DIG antibody (Boehringer Mannheim, Mannheim, Germany). The alkaline phosphatase reaction was developed with 5-bromo-4-chloro-3-indolyl phosphate and nitroblue tetrazolium (Boehringer Mannheim, Mannheim, Germany).

### Antibody generation against the mouse H1oo protein

An anti-H1oo serum was raised by Bethyl Laboratories Inc. (Montgomery, TX) in rabbits against a 30-mer peptide specific for histone H1oo: KRSGSRQEANAHGKTKGETKGEKSKPLASKVQ-NS and affinity purified.

### Immunohistochemistry

Ovarian sections were incubated in a microwave oven for 15 minutes at 500 watts in 0.1 M citrate buffer (pH 6.0) and allowed to cool down for 15 minutes. Immunostaining was performed using the Ventana automated IHC staining system (Ventana Medical Systems, Tucson, AZ) with a DAB (diaminobenzidine) kit. After incubation with an avidin-biotin blocker for 8 minutes, sections were incubated overnight at room temperature with 1.5  $\mu$ g/ml of the affinity-purified primary (rabbit) antibody against mouse H1oo. After washing, the slides were reincubated with a 1:750 dilution of a secondary biotinylated antibody against rabbit IgG (Sigma). The sections were eventually counter stained lightly with Hematoxylin. Negative controls included the use of a nonspecific rabbit IgG and the omission of a secondary antibody.

### Immunofluorescent localization of H1oo

Oocytes and embryos were fixed for 20 minutes at room temperature in a freshly prepared solution of 2% paraformaldehyde in PBS (pH 7.4). The fixed oocytes/embryos were then incubated for 1 hour at room temperature in a blocking solution (0.01 M PBS, 10% goat serum and 0.5% Triton X100). The fixed/blocked oocytes/embryos were then incubated for 1 hour at room temperature with affinity-purified anti-mouse H1oo antibodies (1.0  $\mu$ g/ml) in a dilution buffer solution (0.01 M PBS, and 0.5% Triton X100). Thereafter, the oocytes/embryos were washed three times for 15 minutes in 0.01M PBS, and reincubated with the Alexa Fluor 488 goat anti-rabbit IgG conjugate (Molecular Probes, Eugene, OR; diluted 1:1000) for 1 hour at room temperature. Thereafter, the oocytes/embryos were washed as above and the DNA stained using the Hoechst 33342 dye (Molecular Probes, Eugene, OR). To mount the oocytes/embryos for viewing, a drop of ProLong Antifade mounting media (Molecular Probes, Eugene, OR) was placed on a siliconized glass microscope slide, the oocytes/embryos carefully pipetted into the drop and covered with a glass slip. Samples were examined using an Olympus BX60 microscope (Olympus, Tokyo, Japan) equipped for epifluorescence with appropriate filter sets.

### Western immunoblotting analysis of oocytic and embryonic proteins

Groups of oocytes and embryos were washed in phosphate-buffered saline, extracted in 15  $\mu$ l of protein extraction buffer (50 mM Tris-HCl pH 7.5, 0.5M urea, 2% Nonidet-P40, protease inhibitor cocktail, phosphatase inhibitor cocktail (Sigma), 5% mercaptoethanol and frozen at  $-80^\circ\text{C}$ ). Extracts were resolved on 10% SDS-PAGE gels and blotted onto nitrocellulose membranes. The blots were blocked with 5% non-fat dry milk in 10 mM Tris, 150 mM NaCl, 0.05% Tween 20 (TTBS) for 1 to 2 hours prior to incubation with 0.2  $\mu$ g of the rabbit

anti-mouse H100 antibody. The secondary antibody, conjugated to peroxidase (Amersham Pharmacia, Piscataway, NJ), was diluted 1/1000. The signal was detected by means of the ECL system (Amersham Pharmacia, Piscataway, NJ).

### Statistical analysis

Statistical significance was determined by ANOVA followed by Dunnett's test using the JMP software program (SAS Institute, Cary, NC).  $P < 0.05$  was considered to be significant when compared with the control samples.

### Accession Number

H100, AY007195.

## RESULTS

### SSH identifies an ovary-specific transcript

Individual cDNA inserts generated by SSH were amplified by using PCR primers corresponding to plasmid sequences flanking the multiple cloning site. The individual amplicons were subsequently sequenced and subjected to nucleotide BLAST analysis. Novel clones were designated as such if no significant match (E value  $> e^{-5}$ ) was obtained for the nonredundant database. The ovary-specific expression pattern of one of 83 novel SSH-generated cDNAs (M5H8; 555bp), was validated by Northern blot analysis. Specifically, commercially derived nylon membranes (Origene Technologies, Rockville, MD) containing RNA from 12 different mouse tissues were probed with a radiolabeled/PCR-amplified version of the M5H8 cDNA. As shown in Fig. 1A, the novel clone in question was not expressed in any of the non-ovarian tissues tested. The presence of mRNA on the nylon membrane in question was verified by re-probing for transcripts corresponding to *Gapd*, a housekeeping gene (Fig. 1A).

Phase-specific ovarian expression of the cDNA clone under study was further analyzed by Northern blot analysis. Total RNA isolated from the ovaries of mice at different stages of a simulated ovarian cycle was transferred to nylon membranes and probed with the radiolabeled/PCR-amplified version of the M5H8 cDNA. As shown in Fig. 1B, the relative ovarian expression of *Gapd* persistently exhibited  $>50\%$  reduction as early as 48 hours after the administration of PMSG when compared with the unstimulated state. The transcript size of the gene in question was calculated to be approximately 1.2 kb (Fig. 1B). Equivalent RNA loading was verified by re-probing the same membrane with a probe for  $\beta$ -actin, another housekeeping gene.

### Cloning and structural characterization of H100

The above SSH-generated (555 bp) partial cDNA fragment was used as a probe to screen an ovarian cDNA ( $\lambda$ TriplEx2) library in the hope of isolating a full-length cDNA (1115 bp) clone. Two positive clones, E121 and E82, each containing 1.2 kb inserts, were identified and sequenced (Fig. 2). The sequenced full-length cDNA disclosed a 912 bp open reading frame encoding a putative 34 kDa/304 amino acids protein. Protein BLAST analysis revealed the latter to display a high level of homology to the linker histone B4 of *Xenopus laevis* and to the cs-H1 linker histone of the sea urchin *Parechinus mularis* (Fig. 3). In general, linker histones of the H1 variety possess a three-domain structure, i.e. a central globular

domain flanked by N- and C-terminal tail domains. It is the central globular domain of H1 that interacts with linker DNA, and has thus retained sufficient conservation to allow direct

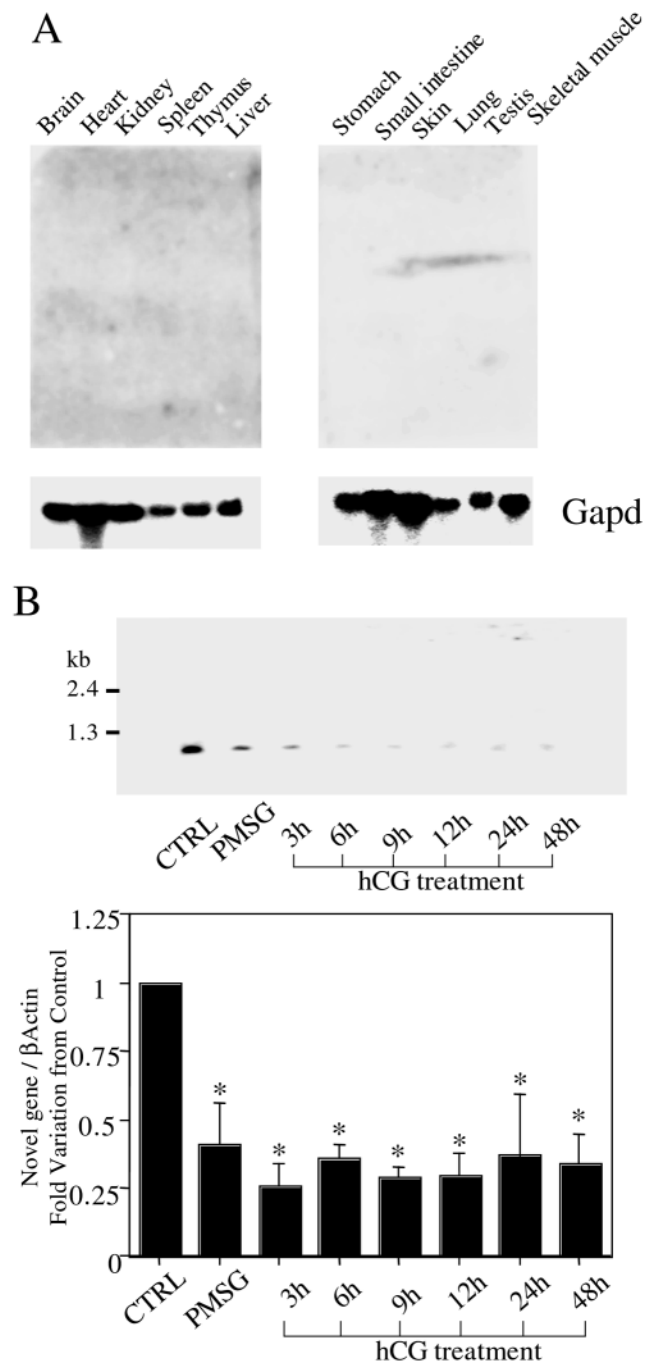


**Fig. 1.** Tissue localization of *H100* transcripts: northern blot analysis. (A) Total RNA (20  $\mu$ g/lane) from brain, heart, kidney, spleen, thymus, liver, stomach, small intestine, skin, lung, testis and skeletal muscle. Hybridization was performed with [ $^{32}$ P]-labeled H100 and *Gapd* cDNA probes. (B) H100/ $\beta$ -actin ratios were calculated and compared with expression in the unstimulated control (CTRL) ovaries. The data from three independent experiments are shown in the graph. \*, statistical significance at  $P < 0.05$  when compared with the CTRL samples. Statistical significance was determined by ANOVA followed by Dunnett's test by using statistical analysis software JMP (SAS Institute, Cary, NC).

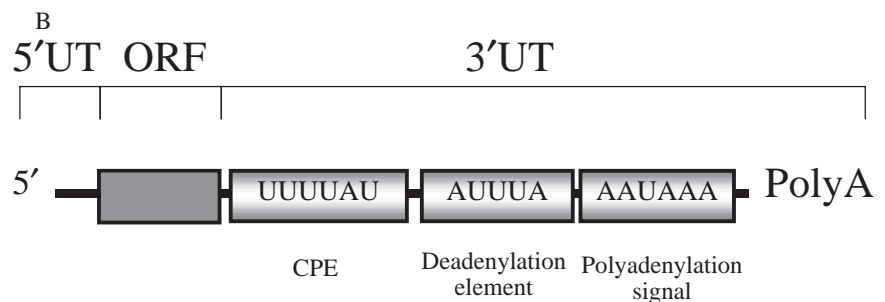
A

```

1  AGCTAACTGAGCGAGCACTGGCCTGGCCTGCTGCTGCCTGTGCCATGGCTCCTGGGAGTGTC
                                     M A P G S V
64  TCCAGTGTTCCTCCTCCTCTTTCCCTCCAGGGACACATCCCCTTCTGGATCATGTGGG
   S S V S S S S F P S R D T S P S G S C G
124 CTCCCTGGAGCTGACAAGCCAGGTCCAAGTTGCCGCGAGAATCCAAGCAGGCCAAAGGAAC
   L P G A D K P G P S C R R I Q A G Q R N
184 CCAACAATGCTGCACATGGTGTAGAGGCTTTGAAGGCCCGGGAGGCACGCCAGGGCACA
   P T M L H M V L E A L K A R E A R Q G T
244 TCAGTTGTAGCCATCAAGGTCTACATCCAACACAAGTACCCGACAGTGGACACCACCCGT
   S V V A I K V Y I Q H K Y P T V D T T R
304 TTCAAGTACCTGTTGAAGCAAGCTCTGGAAACTGGCGTTCGTCGAGGCCCTCCTCACCAGG
   F K Y L L K Q A L E T G V R R G L L T R
364 CCTGCTCACTCCAAGGCCAAGGGTGCCACTGGCAGCTTCAAACACTAGTTCCAAAGCCCAAG
   P A H S K A K G A T G S F K L V P K R K
424 ACAAGAAAAGCCTGTGCCCCCAAAGCCGGCAGGGGAGCTGCAGGTGCCAAGGAGACAGGC
   T K K A C A P K A G R G A A G A K E T G
484 TCCAAGAAATCTGGATTGCTGAAGAAAGACCAAGTTGGCAAGGCCACGATGGAGAAAAGGG
   S K K S G L L K K D Q V G K A T M E K G
544 CAGAAGAGGAGGGCTTACCCTTGCAAGGCAGCCACACTGGAGATGGCACCTAAGAAAGCC
   Q K R R A Y P C K A A T L E M A P K K A
604 AAGGCGAAACCGAAAGAGGTGAGAAGGCTCCCCTAAAACAAGACAAAGCAGCAGGGGCC
   K A K P K E V R K A P L K Q D K A A G A
664 CCTCTGACTGCCAATGGAGGCCAGAAGGTCAAACGCAAGTGGGAGCAGGCCAAGAAGCAAT
   P L T A N G G Q K V K R S G S R Q E A N
724 GCCCATGGGAAAACCAAAGGTGAGAAATCGAAGCCCTGGCCAGCAGGTCCAGATAGC
   A H G K T K G E K S K P L A S K V Q N S
784 GTTGCTTCCCTCGCCAAAAGGAAGATGGCAGACATGGCCACACTGTGACAGTTGTTTCAG
   V A S L A K R K M A D M A H T V T V V Q
844 GGGGCTGAGACAGTACAGGAGACCAAAGTGCCCACTCCTTCCAGGACATAGGACACAAA
   G A E T V Q E T K V P T P S Q D I G H K
904 GTACAACCCATACCTAGGGTCAGGAAGGCAAAGACCCCTGAGAACACTCAGGCCTGAGTT
   V Q P I P R V R K A K T P E N T Q A
964 ACTTCCCAAGACCTCCTCCAAGGCTCCAGCAAGAAGGCTGAGGCTAGTAGCTAGGGCCA
1024 GGGCTGGGAGATGGCGATTCTGAAGCTTTTTATTGCTAATAAGCTGTACAATGTTTAA
1084 TCATAATTTATCAATAAAGACTTTGTATTTCG

```

**Fig. 2.** Nucleotide and deduced amino acid sequence of the mouse E121 clone. (A) The amino acid sequence of H1oo is shown in single letter code below its nucleotide sequence. The longest open reading frame of *H1oo* yielded a deduced amino acid sequence of 304 residues. The polyadenylation signal (single underline), the cytoplasmic polyadenylation element (double underline) and the deadenylation motifs (broken line) are indicated. The consensus amino acid sequence for Cdc2 kinase is in bold. (B) Anatomy of the 3'UTR of *H1oo*.



sequence comparison between species and (to a degree) between somatic H1 histone subtypes. Alignment of the novel mouse protein (termed histone H1oo), the *Xenopus* histone B4, and the sea urchin cs-H1 proteins revealed that the globular domain of H1oo shares 54 and 52% identity with the corresponding region of the above proteins.

While most mRNAs corresponding to somatic H1 histones are not polyadenylated, the *H1oo* mRNA, not unlike that of *B4* and *cs-H1* mRNAs, is likely polyadenylated as judged by the presence of the consensus adenylation sequence signal, AAUAAA, in the 3' untranslated region (UTR) (Fig. 2A,B). The *H1oo* mRNA further features (in its 3' UTR) the cytoplasmic polyadenylation element (CPE, consensus structure of UUUUA<sub>1-2</sub>U), an element likely required for translational activation in the maturing oocyte (De Moor and Richter, 1999; Richter, 1999) (Fig. 2A,B). In contrast, an embryonic-type CPE, which is oligo (U)<sub>12-27</sub> and likely required for polyadenylation during embryogenesis (Richter,

1999), is not present. Finally, we noted an AUUUA motif in the 3'-UTR region, the presumed function of which is to destabilize *H1oo* mRNA (and presumably other maternally derived mRNAs) after egg activation or fertilization (Voeltz and Steitz, 1998; Zubiaga et al., 1995).

NetPhos analysis (Blom et al., 1999) of H1oo predicted phosphorylation of serine residues in the N-terminal domain (X9), the globular domain (X1), and the C-terminal domain (X5). Possible threonine phosphorylation sites may be located in the N-terminal domain (X1), the globular domain (X2) and the C-terminal domain (X3). No predicted tyrosine phosphorylation site was detected in the H1oo sequence. However, putative Cdc2 kinase and RXXS p90<sup>RSK</sup> phosphorylation motifs were identified and localized to Thr<sup>297</sup> as well as to the Ser<sup>20</sup> and Ser<sup>221</sup> residues.

#### ***H1oo* mRNA and protein are expressed in the oocyte**

To localize the expression of *H1oo* within the ovary, we carried

H1oo	1	MAPGSVSSVSSSSFPSSRDTSPSSGSCGLECADKPGPSCRRIQAGQRNPTMLHMVLEALKAR
H1M/B4	1	MAPKKAVAAPLEGNGKE-NAAVKSSKVKVKRKS----IKLVKTSHPPTLSMVVEVLKKN
cs-H1	1	----MSSSDDDVDIENGDASTPS----PKAIKS-----RKTVTSHPKYNDMLTEALKAL
		Helix I
H1oo	61	EARQGTSVVAIKVYIQHKYPTVDITRFKMLLKOALETGVRGRLTRPAHSAKAKGA--TGS
H1M/B4	56	TERKGTSVQAIRTRILSAHPTVDPLRLKELLRTALNKGLEKGLLIRPLNSSATGA--TGR
cs-H1	47	DEKKGASVLAIKHWIIQTYPEVNTTRMKNLLRMAIKRGVBSGLIVRPPKSEECMGAALTGR
		----- Helix II ----- Helix III -----
H1oo	119	FKLVKPKK-TKKACAPKACRGAAQAKETGSKKSSGLLKKDQ-----VCKATME-KGQKR-
H1M/B4	114	FKLAKPVK-TTKACKENVVSENVDPAEQETQKKAPKKEK-----KAKTEKEPKGEK--
cs-H1	107	FKLGKPPKPAKKAEEKKKEKKNVAAGKKKTAKSPTKKKDRKQSDHDFDYEDDTFCSDPD
		-----
H1oo	170	RYPCKAATLEMAPKKAKAPKPKVVRKAPLKQDKAAGAPLTANG-GQVKRSGSRQEANAH
H1M/B4	165	-----TKAVAKKAKEDSDEKPK-VAKS--KDKKBAKEVDKAN----KEAKEVDKANKEAK
cs-H1	167	VCKTTPPYKKNRAKKQPMKPN-SKKAQSRPSSASANATPKPRLSKSRATVRRSKSSQSP
H1oo	229	CKTKGKESKPLASKVQNSVASLAKRKMADMAHTVTVVQCAETVQETKVTTPSQDIGHKVQ
H1M/B4	213	EVDKAPAKPKKAKTEAAKAEAGGCKAKKEPPKAKAKDKVAKQKDSDECAEAVKAGKKGKVV
cs-H1	226	APSKLKSIRKGLASKSPARK-SKSKSPAKPKSKAATTKTSPAATGKAKAKKTVVKKKDKT
H1oo	289	PIPRVRKAKTPENTQA
H1M/B4	273	N-----
cs-H1	285	PTKKAATTKKKINK-

**Fig. 3.** Amino acid sequence alignment of H1oo with histone H1M/B4 and cs-H1. The amino acid sequences of H1M/B4 and cs-H1 were extracted from the GenBank database (histone H1M/B4, Accession Number X13855; cs-H1, Accession Number AAB48830). Identical amino acid residues are shaded black; similar amino acids are shaded gray; unrelated residues are unshaded. The globular domains are underlined (Helix I, II, III).

out in situ hybridization studies using digoxigenin-labeled antisense and sense H1oo cRNA probes and slide-mounted ovarian sections prepared from randomly-cycling adult mice. As shown (Fig. 4), the H1oo mRNA localized exclusively to the oocyte. No hybridization signal was detected for the control sense probe. Further, H1oo mRNA could not be detected in any other ovarian cell type including theca and granulosa cells, although the possibility of a low level of expression in these tissues remains. Instead, H1oo mRNA was detected in the oocytes of follicles at all stages of development at or beyond the primary-secondary follicle stage. With paraffin-embedded

material, a signal corresponding to H1oo mRNA could be detected only at or beyond the secondary follicle stage. However, when snap-frozen material was used, a signal could be detected as early as the primary follicle stage (data not shown). The signal intensity, however, increased markedly with progressively advanced follicular development. Immunohistochemical studies confirmed that the immunoreactive H1oo protein localized solely to the GV of oocytes at or beyond the primary follicle stage (Fig. 4D). No signal was noted in granulosa or theca cells, thereby attesting to the specificity of the antibody used in the face of the

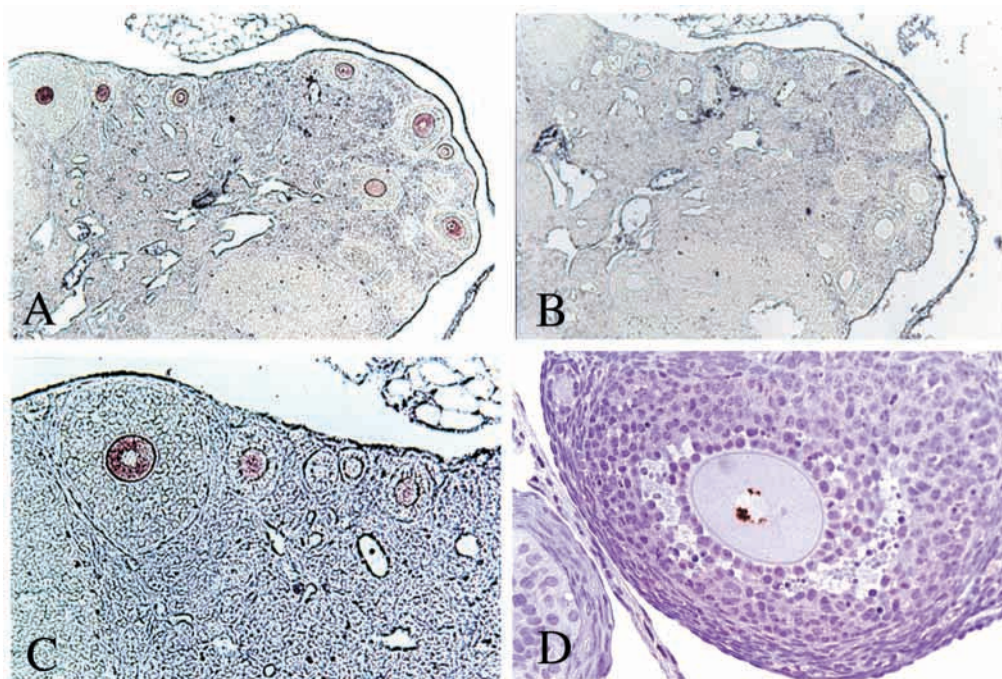


**Fig. 4.** H1oo gene expression in the mouse ovary of 8-week old mice. In situ hybridization with a H1oo DIG-labeled cRNA probe (A-C) and immunohistochemical detection of H1oo protein with H1oo-specific antibody (D). (A) H1oo mRNA localized exclusively to the oocyte. (B) No hybridization was detected for the control sense probe. (C) The signal intensity increased with progressively advanced follicular development. (D) Immunoreactive H1oo protein was solely detected in the nucleus of follicles at the secondary follicle stage.

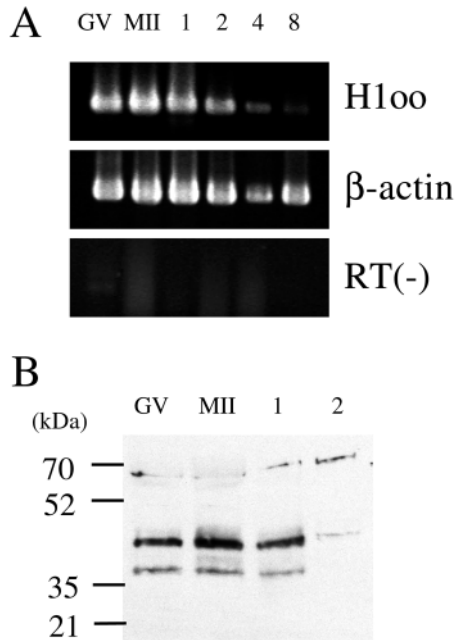


**Fig. 5.** RT-PCR and immunoblot analysis of H1oo during preimplantation development. (A) RT-PCR: cDNA or RNA from 15 oocytes or embryos were used for each reaction. The terms 'GV' and 'MII' corresponds to germinal vesicle stage and metaphase II stage oocyte, respectively. 1, 2, 4 and 8 refer to the number of cells in the developing embryo. A substantial decrease in *H1oo* expression was evident after fertilization.  $\beta$ -actin primers were used as a positive control designed to document the continuous presence of cDNA from embryo lysates. (B) Immunoblotting: protein from 50 oocytes or embryos was subjected to immunoblot analysis for H1oo. H1oo protein levels (42 and 37 kDa) decline rapidly and almost disappear at the two-cell stage (2). The experiments were performed three times with consistent results.

projected presence of somatic linker histone H1 or core histones.

#### Ontogenetic studies of *H1oo* mRNA and protein

*H1oo* mRNA was readily detectable in GV oocytes by RT-PCR (Fig. 5A). After fertilization, however, a substantial decrease was evident in *H1oo* expression. *H1oo* transcripts were all but undetectable at the eight-cell stage embryo. Western blot analysis of H1oo protein in GV oocytes disclosed a major 42 kDa band, as well as a minor 37 kDa band (Fig. 5B). The minor band could reflect a cross-reaction of the antibody with H1oo-related proteins, or partial cleavage, to mention a few hypothetical possibilities. The overall higher molecular weight of H1oo (higher than predicted from the amino acid sequence (34-kDa)) may be compatible with the gel retardation commonly observed for many nuclear histones, owing to their unusual amino acid composition (Burglin et al., 1987). H1oo protein also declined rapidly following fertilization and all but disappeared by the two-cell stage. These results suggest that the *H1oo* transcript was of maternal origin and that it and its encoded protein were promptly degraded following fertilization.

The immunofluorescent detection of H1oo protein in the unfertilized oocyte and the preimplantation embryo is illustrated in Fig. 6. As shown, *H1oo* localized to the intact

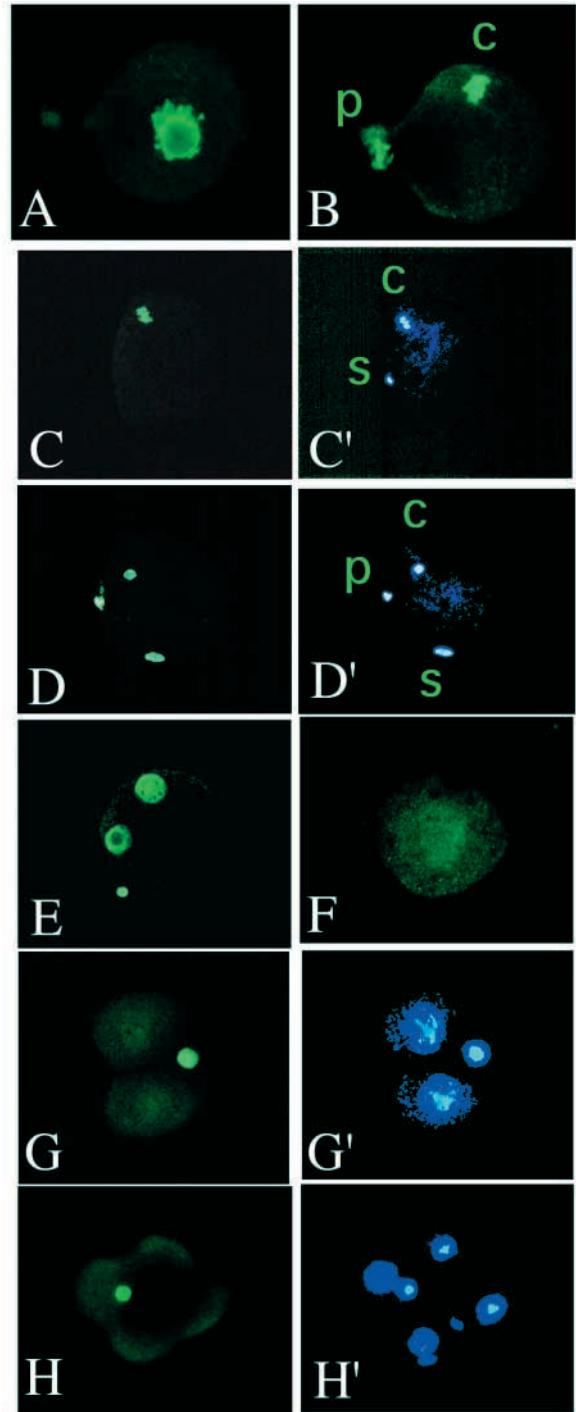


**Fig. 6.** Indirect immunofluorescence of H1oo in oocytes and preimplantation embryos. Anti-H1oo staining (A-C,D,E,F,G,H) and Hoechst 33342 staining (C',D',G',H'). (A) GV stage oocyte. (B) MII stage oocyte; chromatin (c) and first polar body (p). (C,C') One-cell stage embryo just after fertilization; maternal chromatin (c) and sperm head (s). (D,D') One-cell stage embryo; maternal chromatin (c), secondary polar body (p) and sperm head (s). (E,F) One-cell stage embryo. (G,G') Two-cell stage embryo. (H,H') Four-cell stage embryo.

germinal vesicle (GV) of preovulatory oocytes, to the condensed chromosomes of ovulated oocytes arrested at metaphase (M) II, and to the first polar body. Early one-cell

stage embryos (prior to extrusion of the second polar body), featured H100 immunoreactivity in condensed maternal metaphase chromatin but not in the sperm head (Fig. 6C). However, following second polar body extrusion, H100 immunoreactivity was detected in the swollen sperm head as well as in the second polar body (Fig. 6D). The second polar body remained brightly fluorescent throughout early embryogenesis. Nuclear staining, however, was somewhat reduced in two-cell embryos, when compared with the one-cell stage (Fig. 6G). At the four-cell stage of embryonic development, nuclear staining was no longer detectable although, as stated earlier, a strong signal persisted in the second polar body (Fig. 6H).

## DISCUSSION

To date, seven 'somatic' subtypes of H1 linker histones have been identified in mammals. Five of these, collectively termed somatic subtypes, designated H1a, H1b, H1c, H1d and H1e, display significant (60-85%) amino acid identity (Doenecke et al., 1997). A sixth subtype, H1t, is the only 'somatic' subtype that is tissue specific, by virtue of its exclusive expression in primary pachytene spermatocytes during prophase I of meiosis (Drabent et al., 1998). The seventh somatic subtype, H1<sup>0</sup>, in turn, differs from the other H1 varieties. Specifically, it is shorter than most somatic H1 linker histones (190 versus 210 amino acids) and is highly related in sequence and immunochemical properties to the avian red blood cell histone H5 (Doenecke et al., 1997). At the time of this writing, no evidence exists for a mammalian H1 linker histone of the nonsomatic (i.e. oocytic) variety.

Herein we report the cloning of a 1115 bp full-length cDNA from the mouse ovary encoding a novel oocyte-specific linker histone (H100), a 304 amino acid protein with a calculated molecular mass of 34 kDa. Nucleotide Basic Local Alignment Tool (BLAST) analysis of the full-length H100 cDNA against the nonredundant/publicly accessible databases failed to reveal significant homology to previously characterized mammalian genes. However, substantial amino acid sequence homology was registered for the oocyte-specific B4 histone of *Xenopus laevis* and cs-H1 histone of sea urchin. The three proteins displayed the highest degree of sequence identity in their central globular domains. Indeed, the central globular domains of the H100 and B4 histones shared 54% identity.

While most somatic histone H1 mRNAs are not polyadenylated, H100 mRNA, not unlike other (non-mammalian) oocyte-specific linker histones, displayed polyadenylation, putatively mediated by the consensus signal AAUAAA. In addition, the 304 amino acid H100 protein constituted an exceptionally long H1 histone similar to the B4 and cs-H1 proteins of the frog and the sea urchin (273 and 299 amino acids, respectively). These three proteins are the longest H1 histones known to date. These structural data, by themselves, suggest that histone H100 is a mammalian homolog of the oocyte-specific histone B4 of the frog and of the cs-H1 histone of the sea urchin. This contention is further supported by a comparable ontogenetic patterns of expression. Thus, H100 may in fact perform conserved functions (comparable with B4 and cs-H1) during mammalian oogenesis and early embryogenesis.

Cytoplasmic polyadenylation and deadenylation are essential processes that control the translation of maternal mRNAs in the oocyte and the early stage embryo (De Moor and Richter, 1999; Fox et al., 1989; Richter, 1999; Sheets et al., 1994; Stebbins-Boaz et al., 1996; Stebbins-Boaz and Richter, 1994). In maturing *Xenopus* and mouse oocyte, two 3'UTR elements are required to promote polyadenylation and thus translation; the cytoplasmic polyadenylation element (CPE, consensus structure of UUUUA<sub>1-2</sub>U) and the polyadenylation hexanucleotide (AAUAAA) (De Moor and Richter, 1999; Fox et al., 1989; Sheets et al., 1994; Stebbins-Boaz et al., 1996; Stebbins-Boaz and Richter, 1994). The increase in immunoreactive H100 protein from GV to MII is consistent with the presence of such elements in the 3'UTR of H100. In the *Xenopus* embryo, polyadenylated mRNAs may undergo specific *cis* element-directed deadenylation, a process that results in translational repression (Shaw and Kamen, 1986; Stebbins-Boaz and Richter, 1994; Voeltz and Steitz, 1998). The 3'UTR of H100 displays such a *cis* element, i.e. an AUUUA motif that has been shown to be essential for deadenylation during early *Xenopus* development (Voeltz and Steitz, 1998). Polyadenylation during embryogenesis requires the polyadenylation hexanucleotide and an embryonic CPE, which is oligo(U)<sub>12-27</sub> (Richter, 1999). The lack of an embryonic CPE and the presence of an AUUUA motif could explain the rapid decrease in immunoreactive H100 after fertilization.

H100 mRNA was detected in the oocyte of follicles at or beyond the primary follicle stage. However, oocytic H100 transcripts decreased after fertilization. Immunoreactive H100 first appeared at the secondary follicle stage and disappeared at the four-cell stage. The developmentally regulated transition of H100 is thus similar to that reported for the oocyte-specific linker histone B4 of the frog (Dworkin-Rastl et al., 1994; Hock et al., 1993; Smith et al., 1988). This transition is thought to be regulated, at least in part, by post-transcriptional mechanisms such as deadenylation. These results are compatible with the observation that somatic linker histones become undetectable in oocytes shortly after birth, re-emerging yet again at the two-cell embryo stage (Stein and Schultz, 2000).

Our data clearly demonstrate that the H100 protein was detectable from the secondary follicle oocyte to the two-cell stage embryo. What could be the functional significance of this expression pattern? The rate of transcription decreases during oocyte development, as assessed by an Sp1-dependent reporter gene (Worrad et al., 1994) and by endogenous transcription (Brower et al., 1981). This decrease in transcription is correlated with chromosome condensation that occurs during oocyte growth (Debey et al., 1993; Wickramasinghe et al., 1991). H100 may control transcription by changing the structure of chromatin during oocyte development. Recent studies in *Xenopus* have demonstrated that the somatic linker histones function as gene repressors for the oocyte-type 5S RNA genes (Bouvet et al., 1994; Kandolf, 1994). Although the latter observation must be qualified by the absence of functional somatic linker histones in the oocytes, these results imply that the oocyte-specific linker histone may also function as a specific gene repressor.

When an oocyte resumes meiotic maturation, it arrests in metaphase of its second meiotic division, a point at which maternal transcription stops (Bachvarova, 1992). Fertilization



triggers the completion of the second meiotic division and the formation of a one-cell embryo containing a haploid paternal pronucleus derived from the sperm and a haploid maternal pronucleus derived from the oocyte. Although the bulk of both transcription and translation of mouse zygotic genes does not occur until the two-cell stage, early limited transcription in effect begins in late one-cell embryos. This delay in zygotic gene activation is attributed to chromatin remodeling from a condensed meiotic state to one in which select genes can be transcribed while assuring that other genes are not accidentally and prematurely expressed (Nothias et al., 1995; Wiekowski et al., 1997).

Studies over the past decade have identified Mos as the cytostatic factor (MII arresting activity), and mitogen activated protein kinase kinase and p42 mitogen-activated protein kinase (MAPK) as essential mediators of this activity (Sagata, 1997). Recently, the meiotically-activated Mos/MAPK pathway has been shown to cause meiotic arrest at MII through the MAPK-dependent activation of the protein kinase p90 Rsk (Bhatt and Ferrell, 1999; Gross et al., 1999). Indeed, the H100 protein contains potential Rsk-dependent (serine) phosphorylation sites (RXXS) at positions 20 and 221. Given that Mos is capable of promoting the polyadenylation of transcripts corresponding to the *Xenopus* oocyte-specific linker histone B4, one that features Mos-responsive elements in its mRNA (De Moor and Richter, 1997; De Moor and Richter, 1999), it is possible that a functional relationship exists between Mos and H100. Whether phosphorylation of H100 leads to MII meiotic arrest or to transcriptional control of somatic and oocytic genes remains to be determined. After all, Rsk's can phosphorylate a growing list of substrates involved in various cellular processes, such as Bcl-associated death promoter in cell survival, histone H3 in chromatin remodeling and Myt1 in cell cycle regulation (Nebreda and Gavin, 1999).

In summary, H100, a mammalian oocyte-specific linker histone, has been uncovered in an ovary-selective cDNA library. Investigation of possible functional role(s) of H100 is required in order to elucidate the mechanisms underlying its possible control of gene expression before, during or even after fertilization.

We thank Drs Richard M. Schultz, Nava Dekel and John J. Eppig for critical reading of the manuscript. We also acknowledge the expert technical assistance of Emylie Seamen and Nikki Kirkman. This work was supported, in part, by NIH Grants HD30288 and 37845 (E. Y. A.), and The Lalor Foundation Fellowship Award (J. D. H.).

## REFERENCES

- Bachvarova, R. F.** (1992). A maternal tail of poly(A): the long and the short of it. *Cell* **69**, 895-897.
- Bhatt, R. R. and Ferrell, J. E., Jr** (1999). The protein kinase p90 rsk as an essential mediator of cytostatic factor activity. *Science* **286**, 1362-1365.
- Blom, N., Gammeltoft, S. and Brunak, S.** (1999). Sequence and structure-based prediction of eukaryotic protein phosphorylation sites. *J. Mol. Biol.* **294**, 1351-1362.
- Bouvet, P., Dimitrov, S. and Wolffe, A. P.** (1994). Specific regulation of *Xenopus* chromosomal 5S rRNA gene transcription in vivo by histone H1. *Genes Dev.* **8**, 1147-1159.
- Brower, P. T., Gizang, E., Boreen, S. M. and Schultz, R. M.** (1981). Biochemical studies of mammalian oogenesis: synthesis and stability of various classes of RNA during growth of the mouse oocyte in vitro. *Dev. Biol.* **86**, 373-383.
- Burglin, T. R., Mattaj, I. W., Newmeyer, D. D., Zeller, R. and De Robertis, E. M.** (1987). Cloning of nucleoplasmin from *Xenopus laevis* oocytes and analysis of its developmental expression. *Genes Dev.* **1**, 97-107.
- Childs, G., Nocente-McGrath, C., Lieber, T., Holt, C. and Knowles, J. A.** (1982). Sea urchin (*lytechinus pictus*) late-stage histone H3 and H4 genes: characterization and mapping of a clustered but nontandemly linked multigene family. *Cell* **31**, 383-393.
- Clarke, H. J., Bustin, M. and Oblin, C.** (1997). Chromatin modifications during oogenesis in the mouse: removal of somatic subtypes of histone H1 from oocyte chromatin occurs post-natally through a post-transcriptional mechanism. *J. Cell Sci.* **110**, 477-487.
- Clarke, H. J., McLay, D. W. and Mohamed, O. A.** (1998). Linker histone transitions during mammalian oogenesis and embryogenesis. *Dev. Genet* **22**, 17-30.
- Crane-Robinson, C.** (1999). How do linker histones mediate differential gene expression? *BioEssays* **21**, 367-371.
- De Moor, C. H. and Richter, J. D.** (1997). The Mos pathway regulates cytoplasmic polyadenylation in *Xenopus* oocytes. *Mol. Cell. Biol.* **17**, 6419-6426.
- De Moor, C. H. and Richter, J. D.** (1999). Cytoplasmic polyadenylation elements mediate masking and unmasking of cyclin B1 mRNA. *EMBO J.* **18**, 2294-2303.
- Debey, P., Szollosi, M. S., Szollosi, D., Vautier, D., Girousse, A. and Besombes, D.** (1993). Competent mouse oocytes isolated from antral follicles exhibit different chromatin organization and follow different maturation dynamics. *Mol. Reprod. Dev.* **36**, 59-74.
- Dimitrov, S., Dasso, M. C. and Wolffe, A. P.** (1994). Remodeling sperm chromatin in *Xenopus laevis* egg extracts: the role of core histone phosphorylation and linker histone B4 in chromatin assembly. *J. Cell Biol.* **126**, 591-601.
- Dimitrov, S. and Wolffe, A. P.** (1996). Remodeling somatic nuclei in *Xenopus laevis* egg extracts: molecular mechanisms for the selective release of histones H1 and H1(0) from chromatin and the acquisition of transcriptional competence. *EMBO J.* **15**, 5897-5906.
- Doenecke, D., Albig, W., Bode, C., Drabent, B., Franke, K., Gavenis, K. and Witt, O.** (1997). Histones: genetic diversity and tissue-specific gene expression. *Histochem. Cell Biol.* **107**, 1-10.
- Drabent, B., Bode, C., Miosge, N., Herken, R. and Doenecke, D.** (1998). Expression of the mouse histone gene H1t begins at premeiotic stages of spermatogenesis. *Cell Tissue Res.* **291**, 127-132.
- Dworkin-Rastl, E., Kandolf, H. and Smith, R. C.** (1994). The maternal histone H1 variant, H1M (B4 protein), is the predominant H1 histone in *Xenopus* pregastrula embryos. *Dev. Biol.* **161**, 425-439.
- Fox, C. A., Sheets, M. D. and Wickens, M. P.** (1989). Poly(A) addition during maturation of frog oocytes: distinct nuclear and cytoplasmic activities and regulation by the sequence UUUUUU. *Genes Dev.* **3**, 2151-2162.
- Gross, S. D., Schwab, M. S., Lewellyn, A. L. and Maller, J. L.** (1999). Induction of metaphase arrest in cleaving *Xenopus* embryos by the protein kinase p90Rsk. *Science* **286**, 1365-1367.
- Hennebold, J. D., Tanaka, M., Saito, J., Hanson, B. R. and Adashi, E. Y.** (2000). Ovary-selective genes I: The generation and characterization of an ovary-selective complementary deoxyribonucleic acid library. *Endocrinology* **141**, 2725-2734.
- Herlands, L., Allfrey, V. G. and Poccia, D.** (1982). Translational regulation of histone synthesis in the sea urchin *strongylocentrotus purpuratus*. *J. Cell Biol.* **94**, 219-223.
- Hock, R., Moorman, A., Fischer, D. and Scheer, U.** (1993). Absence of somatic histone H1 in oocytes and preblastula embryos of *Xenopus laevis*. *Dev. Biol.* **158**, 510-522.
- Kandolf, H.** (1994). The H1A histone variant is an in vivo repressor of oocyte-type 5S gene transcription in *Xenopus laevis* embryos. *Proc. Natl. Acad. Sci. USA* **91**, 7257-7261.
- Mandl, B., Brandt, W. F., Superti-Furga, G., Graninger, P. G., Birnstiel, M. L. and Busslinger, M.** (1997). The five cleavage-stage (CS) histones of the sea urchin are encoded by a maternally expressed family of replacement histone genes: functional equivalence of the CS H1 and frog H1M (B4) proteins. *Mol. Cell Biol.* **17**, 1189-1200.
- Nebreda, A. R. and Gavin, A. C.** (1999). Perspectives: signal transduction. Cell survival demands some Rsk. *Science* **286**, 1309-1310.
- Nothias, J. Y., Majumder, S., Kaneko, K. J. and DePamphilis, M. L.** (1995). Regulation of gene expression at the beginning of mammalian development. *J. Biol. Chem.* **270**, 22077-22080.
- Richter, J. D.** (1999). Cytoplasmic polyadenylation in development and beyond. *Microbiol. Mol. Biol. Rev.* **63**, 446-456.

- Sagata, N.** (1997). What does Mos do in oocytes and somatic cells? *BioEssays* **19**, 13-21.
- Shaw, G. and Kamen, R.** (1986). A conserved AU sequence from the 3' untranslated region of GM-CSF mRNA mediates selective mRNA degradation. *Cell* **46**, 659-667.
- Sheets, M. D., Fox, C. A., Hunt, T., Vande Woude, G. and Wickens, M.** (1994). The 3'-untranslated regions of c-mos and cyclin mRNAs stimulate translation by regulating cytoplasmic polyadenylation. *Genes Dev.* **8**, 926-938.
- Smith, R. C., Dworkin-Rastl, E. and Dworkin, M. B.** (1988). Expression of a histone H1-like protein is restricted to early *Xenopus* development. *Genes Dev.* **2**, 1284-1295.
- Stebbins-Boaz, B. and Richter, J. D.** (1994). Multiple sequence elements and a maternal mRNA product control cdk2 RNA polyadenylation and translation during early *Xenopus* development. *Mol. Cell. Biol.* **14**, 5870-5880.
- Stebbins-Boaz, B., Hake, L. E. and Richter, J. D.** (1996). CPEB controls the cytoplasmic polyadenylation of cyclin, Cdk2 and c-mos mRNAs and is necessary for oocyte maturation in *Xenopus*. *EMBO J.* **15**, 2582-2592.
- Stein, P. and Schultz, R. M.** (2000). Initiation of a chromatin-based transcriptionally repressive state in the preimplantation mouse embryo: lack of a primary role for expression of somatic histone H1. *Mol. Reprod. Dev.* **55**, 241-248.
- Voeltz, G. K. and Steitz, J. A.** (1998). AUUUA sequences direct mRNA deadenylation uncoupled from decay during *Xenopus* early development. *Mol. Cell. Biol.* **18**, 7537-7545.
- Wickramasinghe, D., Ebert, K. M. and Albertini, D. F.** (1991). Meiotic competence acquisition is associated with the appearance of M-phase characteristics in growing mouse oocytes. *Dev. Biol.* **143**, 162-172.
- Wiekowski, M., Miranda, M., Nothias, J. Y. and DePamphilis, M. L.** (1997). Changes in histone synthesis and modification at the beginning of mouse development correlate with the establishment of chromatin mediated repression of transcription. *J. Cell Sci.* **110**, 1147-1158.
- Wolffe, A.** (1998). *Chromatin*. San Diego: Academic Press.
- Worrad, D. M., Ram, P. T. and Schultz, R. M.** (1994). Regulation of gene expression in the mouse oocyte and early preimplantation embryo: developmental changes in Sp1 and TATA box- binding protein, TBP. *Development* **120**, 2347-2357.
- Zubiaga, A. M., Belasco, J. G. and Greenberg, M. E.** (1995). The nonamer UUAUUUAUU is the key AU-rich sequence motif that mediates mRNA degradation. *Mol. Cell Biol.* **15**, 2219-2230.